Published in final edited form as:
J Nat Prod. 2009 October ; 72(10): 1857–1863. doi:10.1021/np900465e.

Using Enzyme Assays to Evaluate the Structure and Bioactivity of Sponge-Derived Meroterpenes

Sarah J. Robinson[†], **Eric K. Hoobler**[†], **Michelle Riener**[†], **Steven T. Loveridge**[†], **Karen Tenney**[†], **Frederick A. Valeriote**[‡], **Theodore R. Holman**[†], and **Phillip Crews**[†,*]

[†]Department of Chemistry and Biochemistry, University of California Santa Cruz, Santa Cruz, California 95064

[‡]Josephine Ford Cancer Center, Henry Ford Health System, Detroit, Michigan 48202

Abstract

Enzyme screening of crude sponge extracts prioritized a 2005 Papua New Guinea collection of *Hyrtios* sp. for further study. The MeOH extract contained puupehenone and four puupehenone analogs (**1, 2, 3, 5**, and **7**) along with a new diastereomer, 20-epi-hydroxyhaterumadienone (**4**) and a new analog 15-oxo-puupehenoic acid (**6**). The drimane terpene core of **4** and **6** was rapidly dereplicated, and modified Mosher's method identified **4** while 1D and 2D NMR techniques were used to solve **6**. These compounds plus noteworthy repository natural products and standards were tested against three lipoxygenase isozymes, human 5-, 12- and 15-lipoxygenases. Significant potency and selectivity profiles were exhibited in the human 5-lipoxygenase assay by puupehenone (**1**) and jaspaquinol (**9**) and structural factors responsible for activity identified.

In recent years our quest to exploit sponge-derived scaffolds has been guided by four types of screening paradigms. These range from (a) employing LC-MS to guide isolation of major and minor metabolites,1 (b) using cell-based primary screens to detect compounds selective against solid tumors,2 (c) probing for disruption of protein-protein interactions (PPI) between Bcl-2 family proteins with the pro-survival BH3-domain binding proteins,3 and (d) challenging enzyme targets relevant to anticancer therapeutic lead discovery.4 The work described herein initially began using paradigm (d) against histone deacetylase (HDAC). Our focus first involved a repository extract hit, suspected to contain meroterpenes that were active against class I HDAC enzymes; subsequently it shifted to profiling selected meroterpenoids challenged with human 5-lipoxygenase (5-hLO). The sponge extract of a *Hyrtios* sp. (coll. no. 05409 from Papua New Guinea) was active (IC_{50} < 0.08 μg/mL) in the former screen and a mini-library of meroterpenes displayed activity (at μM levels) in the latter. HDAC is recognized as a validated target in screening programs and inhibitors of its various isoforms are showing promise as chemotherapeutics for solid tumor and hematologic malignancy.5 Especially significant is suberoylanilide hydroxamic acid (SAHA, Vorinostat, Zolinza) which represents the first FDA approved drug to treat advanced cutaneous T-cell lymphoma via HDAC inhibiton.6 Similarly, 5-hLO is emerging as a significant enzyme target for chemotherapeutic intercession in a number of diseases.7 One FDA approved drug for the treatment of asthma via 5-hLO inhibition is zileuton (Zyflo).8 The goal of this project was: (1) to isolate, characterize and screen the bioactive constituents of the extract, and (2) identify compounds from our repository demonstrating selectivity for 5-hLO in a panel including 12- and 15-hLO isozymes. Our findings are reported below.

[*]To whom correspondence should be addressed. Tel: 831-459-2603. Fax: 831-459-2935. phil@chemistry.ucsc.edu.

Results and Discussion

Before launching the drive to characterize the constituents of the active *Hyrtios* MeOH extract, it was essential to map out an approach involving aggressive dereplication. Our two prior evaluations of the bioactive products of *Hyrtios* sp. collections, with similar morphological properties to those of the organism under investigation, utilized sponges from different Indo-Pacific sites including Papua New Guinea (coll. no. 99140)[9] and Indonesia (coll. no. 95653).10 In both cases we observed these extracts to be prolific in their content of puupehenone analogs. In this regard, the haterumadienone11 family represents another related biosynthetic skeleton. Overall, as first pointed out by Scheuer,12 such compounds have conserved ABC rings comprised of a drimane fused to a oxygenated shikimate (**DOS**, Figure 1). We have found that such compounds can be quickly recognized in crude extracts by the NMR signature peaks for the four methyl groups attached to quaternary sites as illustrated in Figure 1. Two other important facts are as follows: (1) the absolute configuration of the **DOS** terpene core has been established as 5*S*, 8*S*, 9*R*, 10*S*[13] and (2) the puupehenone family (see **1**) differs from the haterumadienone class (see **3**) by the size of the carbocyclic D ring, C_6 in the former and C_5 in the latter.

The above background plus our prior experience with extracts containing puupehenone analogs provided the basis for the design of the subsequent isolation and dereplication efforts of new and known puupehenone / haterumadienone compounds. Eventually we discovered that the D ring was the locus for unprecedented substitution patterns. The core **DOS** $\delta_{C,H}$ chemical shifts were used to interrogate each of the metabolites during the purification process as shown in Figure 2 (see also Figure S18, Supporting Information). The known puupehenones were easily identified using the signature NMR data of Figure 1 accompanied by an analysis of their molecular formulas established by ESITOFMS. The CH_2Cl_2 soluble MeOH extract (coded FD) contained puupehenone (**1**) (*m/z* 329.2033 $[M+H]^+$, $C_{21}H_{29}O_3$),[12] 15,20-dimethoxypuupehenol (**2**) (*m/z* 375.2456 $[M+H]^+$, $C_{23}H_{35}O_4$),[10] 20-hydroxyhaterumadienone (**3**) (*m/z* 317.2110 $[M+H]^+$, $C_{20}H_{29}O_3$),[14] a new diastereomer 20-epi-hydroxyhaterumadienone (**4**) (*m/z* 317.2112 $[M+H]^+$, $C_{20}H_{28}O_3$), puupehedione (**5**) (*m/z* 327.1889 $[M+H]^+$, $C_{21}H_{27}O_3$),[15] a new analog identified as compound **6** (*m/z* 357.2107 $[M+H]^+$, $C_{22}H_{29}O_4$) and dipuupehetriol (**7**) (*m/z* 655.3922 $[M+H]^+$, $C_{42}H_{55}O_6$).[16] Structures of the known compounds were established by rigorous comparison of their NMR and MS properties to those in the literature.

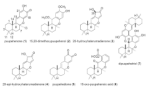

Initially a compound having the framework consistent with known 20-hydroxyhaterumadienone (**3**)[14] was isolated from the FD fraction coded as L2 (28.4 mg, see Figure S18, Supporting Information). However, it was isolated as a mixture containing a new diastereomer (deduced by MS formula analysis as shown above) ultimately concluded to be **4**. A clearer view of this circumstance was obtained by the ^1H NMR spectrum of the sample obtained from a second chromatographic step, coded as FD L2 H5, shown in Figure 3, emphasizing the doubling of signals for H-15, H-18 and H-20, in relative proportions of 2:1. The final purification of this fraction required chiral chromatography to afford **3** (5.1 mg) and **4** (2.5 mg).

Supporting Information Available: ^1H, ^{13}C, gCOSY, gHMBC, and gHMQC NMR data for **6** and MS data and ^1H, ^{13}C and MS data for **4** along with an isolation scheme for **1, 2, 3, 4, 5, 6**, and **7** and a table of puupehenone bioactivities are provided free of charge via the Internet at http://pubs.acs.org. Also free at this website is a database of select puupehenone bioactivities and optical rotations.

The low field region of the ^{1}H NMR spectrum of **3** and **4** showed the greatest difference in shifts between isostructural protons, therefore it was assumed that their configuration differences were at C-20 rather than at C-8 or C-9. If this assumption was correct, then we could determine the absolute configuration at C-20 in each diastereomer by application of the modified Mosher's method.[17, 18] Derivatization of **3** with (*R*) and (*S*)-(+)-α-methoxy-α-trifluoromethylphenylacetyl chloride ((*R*) and (*S*)-MTPA-Cl) afforded *S*-MTPA-**3** (**3'**) and *R*-MTPA-**3** (**3"**) respectively, as seen in Figure 4; and a similar treatment of **4** provided **4'** and **4"**. Surprisingly, the straightforward analysis of $\Delta\delta^{SR}$ data shown in Figure 4 (also see Figures S13, Supporting Information) could not be completed until an error in the literature for **3a'** (= our **3'**) and **3a"** (= our **3"**) was corrected as now shown in Figure 4·[14] The error was resolved by accurate correlation, using gHMQC NMR data, of the low field δ_H values for all four compounds (**3**', **3**", **4'**, **4**", Figures S19 – S23, Supporting Information) to their correct structural positions. The assembled data supported the conclusions that **3** possessed the 20*R* configuration and **4** was the new 20*S* analog. NOESY data observed between H-3 (ax) to H-5 to H-9 to H_3-13 confirmed the same ABC ring relative configuration between **1** and **4**. This data, plus the fact that **3** and **4** were isolated with puupehenone (**1**), led to the assumption that all had identical absolute chirality for the ABC rings.[14]

The second new compound to be isolated, **6**, was initially obtained in small amounts from FD partition chromatographic fractions (see Figure S18 Supporting Information), coded FD L5 H2 (0.6 mg) and FD L6 H2 (0.3 mg). A much larger sample was obtained from the more polar partition fractions (coded MW leading to the fraction coded FM). It took two rounds of HPLC to yield FM P10 H9 (14.9 mg) clearly containing **6** as evidenced by the 1,2,3-trisubstituted benzene D ring ^{1}H NMR signals shown in Table 1; consisting of resonances at δ 7.48 (dd, 8, 7.5 Hz), δ 7.27 (dd, 7.5, 1.5 Hz), and δ 7.01 (dd, 8, 1.5 Hz). In addition, the NMR shifts (δ_C and δ_H) for **6** were nearly identical to those of the known 15-oxo-puupehenol (**8**)[15] for the ABC rings and their corresponding substituents. This observation established both the framework and relative configurations of all moieties in this portion of the structure. Also evident from a plot of Δδ shift differences for **6** vs. **8** in Figure 5 was that the locus of structural differences seemed confined to the D ring. Supporting this conclusion were additional relationships for B, C, and D ring residues of **6** established through gHMBC correlations from H-9 (δ_H 2.04) to C-15 (δ_C 196.2) and to C-16 (δ_C 119.2).

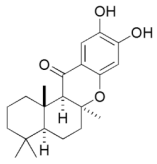

15-oxo-puupehenol (**8**)

The final step in establishing structure **6** involved defining the carboxylate residue and its environment relative to the D ring. The two possible sets of substructures are shown in Figure 6 and consisted of: (a) **6I** and **6II** or (b) **6III** and **6IV**. The assignments of δ_c's alongside each of the structures were based on gHMBC results rather than chemical shift analogies to model compounds. One anchor point for this process was the array consisting of the aromatic AMX pattern protons. A second element involved establishing the relative proximity of carbons separated by two to four bonds with specific H-C correlations including: (a): from H-7ax (δ_H 2.04) to δ_C 161, and (b) from H-Ar (δ_H 7.27) to δ_C 172. Four distinct $^{2, 3}J$ gHMBC correlations were used (see Figure 5 and Table 1) and only substructure **6II** was consistent with these data. Finally, the *trans-cis* fused ABC ring junction proposed above was confirmed by the NOESY data (shown in Table 1) and absolute configurations shown here for **6** were based on the biosynthetic analogy to **1**, noted above.

At completion of the purifications and characterizations of compounds **1 – 7** (see Figure 2), efforts were made to subject these samples to the HDAC inhibition assay. Unfortunately, the overall outcome was incomplete due to the discontinuation of the assay by our therapeutics collaborators and disparate Biomol Kit test results. Examples of the positive HDAC inhibition activities observed on chromatographic fractions are as follows: (a) the fraction coded L2 (28.4 mg) containing **1** (1.9 mg), **3** (5.1 mg), and **4** (2.5 mg) exhibited IC_{50} = 7 μg/mL; (b) the fraction coded L3 (30.0 mg), a source of **2** (0.7 mg) and a mixture of **3** and **4** (0.2 mg) exhibited IC_{50} = 3 μg/mL; (c) the fraction coded as L4 (52 mg) afforded **1** (6.2 mg) and **2** (0.9 mg) exhibited IC_{50} = 2 μg/mL; and (d) the fraction coded L5 (151.8 mg) consisting of 95 % pure puupehenone (**1**) (11.6 mg, from partial chromatography) exhibited IC_{50} = 0.9 μg/mL. Recognizing that there are possible complications from impurities, these data collectively indicate that the puupehenone core in **1** may be a reasonably active HDAC inhibitor. However, as noted above no follow-up assay data was obtained on the pure compounds.

We then turned to selecting meroterpenoids from our repository to accompany the compounds isolated above in a further survey using a panel of hLOs. The goal was to identify compounds that might be especially potent and/or selective against the panel of three hLO isoforms. Two new developments were represented in our redesigned hLO evaluation. Firstly, the lipoxygenase assay was altered to flag compounds that were promiscuous inhibitors. This involved the testing of effects in the presence of detergent (Triton X100). Secondly, a new assay arm involved 5-hLO in addition to 12- and 15-hLOs.

Overall, eight compounds were tested and the results appear in Table 2. These are as follows: Set I (puupehenone and analogs): **1** (previous IC_{50} [μM] 15-hLO = 0.8; 12-hLO = 8.3),[9] **3, 5, 6**; Set II (sesterterpenes from the repository) jaspaquinol (**9,** previous IC_{50} [μM] 15-hLO = 0.3; 12-hLO = 4.5),[9] jaspic acid (**10,** previous IC_{50} [μM] 15-hLO = 1.4; 12-hLO = 0.7),[9] and isojaspic acid (**11,** previous IC_{50} [μM] 15-hLO = 5.3; 12-hLO = 3.1)[19]; and Set III (standards) NDGA (**12**, previous IC_{50} [μM] 15-hLO = 0.6; 12-hLO = 42).[9] The standard **12** exhibited the expected behavior of potency and selectivity ratios (54 and 11 shown in Table 2) in the hLO panel.[20, 21] The literature data for zileuton (**13,** Zyflo),[20] not tested here, but an FDA approved therapy for the treatment of asthma via 5-hLO inhibition, provides an important reference point. Encouraging potency and selectivity profiles were exhibited in the 5-hLO assay by puupehenone (**1**) and jaspaquinol (**9**). Firstly, **9** exhibited outstanding selectivity for 5-hLO vs. 12-hLO (ratio > 111 fold) and very good selectivity vs. 15-hLO (ratio = 42), while **1** exhibited very good selectivity for 5-hLO vs. 12-hLO (ratio = 32) but less selectivity vs. 15-hLO (ratio = 9). Second, we revisited our previous hypothesis and experimental evidence that suggested **1, 9** and **12** were reductive LO inhibitors.[20, 21] The new data obtained here support this hypothesis for **9** and **12**, but add an additional perspective of **1**. The difference in 5-hLO potency for **1** and its oxidized analog **5** presents a pattern expected for reductive inhibitors and adds support to our previous hypothesis.[20, 21] However, the identical potency profile observed for this pair against 12-hLO and 5-hLO is unexpected and suggests additional mechanisms may be operating. Furthermore, the new data indicate that structural factors beyond those present in the **DOS** framework of Figure 1 are essential for activity as shown by the inactivity of **3** and **6**. The circumstance of isojaspic acid (**11**) being slightly less potent than jaspic acid (**10**), seems directly a function of the change in relative configuration of the fused decalene ring. Finally, in the cases **1, 9, 10**, and **11**, the addition of Triton X100 lowers potency (data from this study (Table 2) vs. our previous work noted above), possibly due to the formation of aggregates that non-specifically inhibit the hLOs. As a different observation, **1** exhibited modest selectivity against solid tumor cells (human lung adenocarcinoma cells over human leukemic lymphoid cells) in the soft agar disk diffusion assay (DDA, Table S4, Supporting Information).

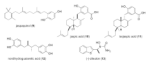

There are several conclusions to be drawn from this study. Interestingly, no new puupehenone analogs have been reported in the last five years. The new compound isolated here expands the list of such frameworks to a total count of 17.[22] Widespread interest in puupehenones has driven a range of biological activity studies that have been accompanied by the development of synthetic strategies to access this structurally interesting chemotype (Table S1, Supporting Information).[23–31] In the future we plan, by semi-synthesis, to create potentially even more selective 5-hLO inhibitors by fusing the structures of puupehenone (**1**) and jaspaquinol (**9**) through their shikimate residues.

Experimental Section

General Experimental Procedures

The optical rotations were determined on a Jasco DIP 370 polarimeter. UV data was obtained on an Agilent 8453 UV/Vis spectrophotometer and IR data was collected on a Perkin-Elmer Spectrum One FTIR spectrometer. All NMR spectra were recorded in $CDCl_3$ at 600 MHz with a 5 mm triple resonance (HCN) cold probe. Chemical shifts are reported in ppm relative to $CDCl_3$ (δ_H 7.27 and δ_C 77.2). Low- and high-resolution mass measurements were obtained by ESI-TOF mass spectrometry. Preparative separation was carried out two ways: (1) Utilizing a Shimadzu SCL-1014 system controller, Shimadzu LC-8A pumps with a Phenomenex Synergy RP 10 μm column, 250 × 21.2 mm. Peak detection employed a Sedex 75 evaporative light scattering detector (ELSD) with fraction collection into disposable culture tubes (25 × 150 mm) using a Gilson 215 liquid handler (Figure S14, Supporting Information). Concurrent MS data was collected on an Applied Biosystems Mariner Biospectrometry Workstation. (2) Using a Waters 600E system controller and pumps with a Prep LC 25 mm radial compression column using 25 × 100 mm C18 Nova-Pak HR16 (6 μm) cartridges. Peak detection utilized both ELSD and UV (254 nm). Semipreparative RP HPLC employed a Phenomenex Synergy Hydro-RP 4 μm column, 10 × 250 mm and UV detection (254 nm). Chiral chromatography utilized a Diacel Chemical Industries Chiracel OJ-RH 5 μm column (150 × 4.6 mm ID).

Animal Material

The *Hyrtios* sp. (UCSC coll. no. 05409, 2 kg wet weight) was collected by SCUBA in November 2005 at Pocklington Reef (10°48.074’ S, 155°44.621’ E), between 60 - 45 feet on a reef wall. The taxonomic identification of *Hyrtios* sp. (POR 3407) was performed by Dr. Nicole J. de Voogd, curator of the National Museum of Natural History in Leiden, The Netherlands. The animal had a pale yellow interior with a brown/yellow exterior, was dense and massive with tubes and had a finely conulose surface with numerous complex oscules. These properties are comparable to those described in literature.[32] Pictures and voucher specimens are available from the corresponding author (P.C.).

Extraction and Isolation

The sponge material was preserved in the field according to our standard procedure,[33] transported back to the laboratory at ambient temperature and stored at 4 °C until processing. Preliminary extraction under high pressure (1500 psi) at 100 °C (ASE apparatus) was performed on approximately 100 g of lightly chopped, dried sponge using hexanes (268 mg), then CH_2Cl_2 (245 mg), and lastly MeOH (602 mg). The MeOH extract demonstrated bioactivity in the HDAC enzyme assay (IC_{50} < 0.08 μg/mL) but the hexanes and CH_2Cl_2 extracts did not.

The remaining animal material was dried, cut into pieces and extracted at room temperature by soaking overnight in MeOH (1 L) three times. The crude MeOH extract (7.8813 g, Figure S18, Supporting Information) was partitioned between MeOH-H_2O (9:1) (coded MW, 4.8155 g) and CH_2Cl_2 (coded FD, 2.5658 g). The ELSD guided preparative RP separation of the FD partition afforded 20 × 50 mL fractions (coded L1 – L20) collected over a linear 45 minute gradient (40 – 100% CH_3CN – H_2O with 0.1% formic acid (FA)) followed by 15 min elution with 100% CH_3CN (flow rate 20 mL/min). Semipreparative RP HPLC fractionation of the fraction coded FD L2 over a linear 25 min gradient (50 – 100% CH_3CN – H_2O with 0.1% FA) afforded **1** (1.9 mg, FD L2 H6) and a mixture of **3** and **4** (11.0 mg, FD L2 H5). This mixture was subjected to semipreparative RP chiral chromatography (60 – 80% CH_3CN – H_2O with 0.1% FA, 40 min) to separate **3** (5.1 mg, FD L2 H5 H2) and **4** (2.5 mg, FD L2 H5 H1). Fraction FD L3 was processed via RP HPLC (65–95% CH_3CN – H_2O, 0.1% FA, 30 min) into seven fractions (H1 – H7), two of these included **2** (0.7 mg, FD L3 H6) and a mixture of **3** and **4** (0.2 mg, FD L3 H7). Fractionation of FD L4 (75–100% CH_3CN – H_2O with 0.1% FA, 30 min) gave nine fractions (H1 – H9) by RP HPLC affording **1** (6.2 mg, FD L4 H8) and **2** (0.9 mg, FD L4 H4). In a similar fashion FD L5 gave seven fractions (H1 – H7, 85–100% CH_3CN – H_2O with 0.1% FA over 25 min) including **1** (11.6 mg, FD L5 H4) and **6** (0.6 mg, FD L5 H2). Next FD L6 gave **5** (1.0 mg, FD L6 H3) and **6** (0.3 mg, FD L6 H2) via RP HPLC over a 25 minute linear gradient (85–100% CH_3CN – H_2O, 0.1% FA). Purification of fraction FD L16 (97–100% CH_3CN – H_2O with 0.1% FA over 10 min followed by 100% CH_3CN for 15 min) afforded **7** (5.7 mg, FD L16 H7). The process to obtain additional **6** (Figure S18) was as follows: MW (4.8155 g) was partitioned between 1:1 nBuOH-H_2O into FM (1.8869 g) and FW (2.5210 g) respectively and FM separated into 10 fractions via RP HPLC (40–100% CH_3CN – H_2O 0.1% FA, 45 m, 10 mL/min). Next fraction 05409 FM P10 (24.9 mg) was separated into 10 fractions (75–100% 8:2 MeOH:CH_3CN – H_2O, 36 min) to afford **6** (14.9 mg, FM P10 H9). In summary five known compounds were obtained and dereplicated by comparing their properties to those in literature: **1**[12], **2**[10], **3**[14], **5**[16], and **7**[16].

HDAC Assays

Fractions L1 – L20 (Figure S18) were evaluated using the HDAC Fluorimetric Assay/Drug Discovery Kit (AK500 Kit, Biomol Research Laboratories, Plymouth Meeting, PA). The HeLa cell nuclear extract, which contained a mixture of nuclear factors and HDAC isozymes, was used as the source of HDAC enzymes. The final substrate concentration was 30 μM and the positive control was trichostatin A (50 nM, 5 nM and 0.5 nM). The incubation (30 min, 37 °C) was terminated with the addition of 50 μL of developer. The assays vessels were black, clear bottom polystyrene 384 well plates and data collection employed a Wallac Victor2 V 1420 Multilabel HTS Counter fluorescence plate reader with excitation wavelength 360 nm and emission wavelength 450 nm.

Disk Diffusion Assay

The soft agar disk diffusion assay was performed using published protocols.[34]

20-Epi-hydroxyhaterumadienone (4)

white solid (2.5 mg); $[\alpha]_D^{27} = -62$ (*c* 0.28, $CHCl_3$); UV (MeOH) λ_{max} (log ε): 201 (3.45), 284 (3.75) nm; IR (NaCl) υ_{max} 3328, 2922, 1563, 1421, 1196 cm^{-1}; ^1H NMR and ^{13}C NMR (see Table S2); HRESIMS $[M + H]^+$ *m/z* 317.2113 (calcd for $C_{20}H_{29}O_3$, 317.2111).

15-Oxo-puupehenoic acid (6)

white solid (14.9 mg); $[\alpha]_D^{27} = +27$ (*c* 0.1, $CHCl_3$); UV (MeOH) λ_{max} (log ε): 216 (4.14), 265 (3.52), 331 (3.23) nm; IR (NaCl) υ_{max} 3492, 2925, 1679, 1594, 1476, 1437, 1285, 1020

cm^{-1}; ^1H NMR and ^{13}C NMR (see Table 1); HRESIMS $[M + H]^+$ *m/z* 357.2107 (calcd for $C_{22}H_{29}O_4$, 357.2060).

Reaction of 3 to Form 3' and 3"

To a solution of **3** (0.5 mg, 1.6 μmol) in pyridine (0.1 mL) (−)-*R*-MTPA-Cl (24 mg, 96 μmol) was added. The mixture was stirred at rt for 2 h and quenched with MeOH (0.2 mL). Water (0.2 mL) was then added and the mixture was extracted with EtOAc (1 mL × 3). The organic phase was dried and concentrated in vacuo. $CDCl_3$ was added (300 μL) to **3'** and directly examined by ^1H (Figure S22, Supporting Information) and gHMQC (Figure S19, Supporting Information) NMR at 600 MHz in a $CDCl_3$ Shigemi tube. Using the same procedure described above, **3"** was obtained from the reaction between (+)-(*S*)-MTPA chloride (24 mg, 96 μmol) and **3** (0.25 mg, 0.8 μmol) in pyridine (0.1 mL) and evaluated with ^1H (Figure S22, Supporting Information) and gHMQC (Figure S20, Supporting Information) NMR.

Reaction of 4 to Form 4' and 4"

To a solution of **4** (0.25 mg, 0.8 μmol) in pyridine (0.1 mL) was added (−)-(*R*)-MTPA chloride (24 mg, 96 μmol). The mixture was stirred at rt for 2 h and quenched with MeOH (0.2 mL). H_2O (0.2 mL) was then added and the mixture was extracted with EtOAc (1 mL × 3). The organic phase was dried and concentrated in vacuo. $CDCl_3$ was added (300 μL) to **4'** and examined by ^1H and gHMQC NMR techniques in a Shigemi tube ($CDCl_3$-type, 600 MHz, Figures S21 and S23, Supporting Information). Using the same procedure as described above, **4"** was obtained from the reaction between (+)-(*S*)-MTPA chloride (24 mg, 96 μmol) and **4** (0.25 mg, 0.8 μmol) in pyridine (0.1 mL) and evaluated by ^1H and gHMQC NMR (Figures S21 and S23, Supporting Information).

Overexpression and Purification of Human Reticulocyte 15-Lipoxygenase-1, Human Platelet 12-Lipoxygenase and Human 5-Lipoxygenase

Human reticulocyte 15-lipoxygenase-1 (15-hLO-1) and human platelet 12-lipoxygenase (12-hLO) were expressed as N-terminally, His6-tagged proteins and purified to greater than 90% purity, as evaluated by sodium dodecyl sulfate-polyacrylamide gel electrophoresis (SDS-PAGE) analysis.[9, 35] Human 5-lipoxygenase (5-hLO) in a pET21 expression vector was received from the Tatulian Lab (University of Central Florida).[36] It was transformed into *E. coli* BL21-DE3 and grown overnight in LB medium (50 mL) with 0.1 mg/mL Ampicillin at 25 °C. Next, the 50 mL growth mixture was separated into 7 × 2 L flasks of media and grown at 30 °C until the OD_{600} reached 0.6. The cells were then induced with 0.25 mM IPTG, followed by lowering the temperature to 18 °C. The cells were harvested 16 – 20 hours post-induction by pelleting at 5,000 g (10 min) and stored at −80 °C until purification.

The frozen cell pellet was resuspended in buffer A (10 mM β-mercaptoethanol, 0.1 mM EDTA, and 50 mM triethanolamine (pH 7.3)) and placed on ice. Cells were lysed using a Power Laboratory Press and cleared by spinning at 40,000 g (25 min). Proteins in the supernatant were precipitated at 50% saturated ammonium sulfate and spun at 40,000 g (25 min). Proteins in the salt pellet can be stored under liquid nitrogen with negligible loss of 5-hLO activity for over 6 months. The salt pellets were resuspended in buffer A for use in activity assays.

Lipoxygenase Assay

The enzyme activity was determined by direct measurement of the product formation following the increase of absorbance at 234 nm using a Perkin-Elmer Lambda 40 UV/Vis spectrometer (25 mM HEPES (pH 8), 0.01% Triton X100, 3 μM arachidonic acid for 12-

hLO, 25 mM HEPES (pH 7.5), 0.01% Triton X100, 3 μM arachidonic acid for 15-hLO-1, and 25 mM HEPES (pH 7.3), 0.3 mM $CaCl_2$, 0.1 mM EDTA, 0.2 mM ATP, 0.01% Triton X100, 10 μM arachidonic acid for 5-hLO). All reactions were performed in 2 mL of buffer and constantly stirred with a rotating stir bar (22 °C). IC_{50} values were determined by measuring the enzymatic rate at a variety of inhibitor concentrations (depending on the inhibitor potency) and plotting their values vs. inhibitor concentration. The corresponding data were fitted to a saturation curve using KaleidaGraph (Synergy), and the inhibitor concentration at 50% activity was determined (IC_{50}). The inhibitors were dissolved in MeOH or DMSO and the corresponding control reactions subtracted from the inhibition data.

Acknowledgments

This work was supported by grants from the NIH [RO1 CA 047135 (PC), U19 CA52955 (PC) and GM56062 (TRH)], NMR equipment grants NSF CHE 0342912 and NIH S10 RR19918, and MS equipment grant NIH S10-RR20939. M. R. was supported by NIGMS (MARC, GM007910-29). Thanks to Novartis Institutes for Biomedical Research (Catherine Fiorilla) for their HDAC inhibition screening. Thanks to L. Matainaho and the government of Papua New Guinea for collection permit support and continued collaboration. Thanks to Captain C. de Wit and Crew of the *M. V. Golden Dawn* for their assistance in sponge collection. Thanks to Dr. R. W. M. van Soest and Dr. N. J. de Voogd for continued assistance in sponge taxonomic identification.

References and Notes

1. Wegerski CJ, Hammond J, Tenney K, Matainaho T, Crews P. J. Nat. Prod 2007;70:89–94. [PubMed: 17253855]
2. Johnson TATK, Cichewicz RH, Morinaka BI, White KN, Amagata T, Subramanian B, Media J, Mooberry SL, Valeriote FA, Crews P. J. Med. Chem 2007;50:3795–3803. [PubMed: 17622130]
3. Calcul L, Chow R, Oliver AG, Tenney K, White KN, Wood AW, Fiorilla C, Crews P. J. Nat. Prod 2009;72:443–449. [PubMed: 19323567]
4. Deschamps JD, Gautschi JT, Whitman S, Johnson TA, Gassner NC, Crews P, Holman TR. Bioorg. Med. Chem 2007;15:6900–6908. [PubMed: 17826100]
5. Marks PA, Rifkind RA, Richon VM, Breslow R, Miller T, Kelly WK. Nat. Rev. Cancer 2001;1:194–202. [PubMed: 11902574]
6. Grant S, Easley C, Kirkpatrick P. Nat. Rev. Drug Discovery 2007;6:21–22.
7. Lewis RA, Austen KF, Soberman RJ. New Engl. J. Med 1990;323:645–655. [PubMed: 2166915]
8. Bell RL, Young PR, Albert D, Lanni C, Summers JB, Brooks DW, Rubin P, Carter GW. Int. J. Immunopharmac 1992;14:505–510.
9. Amagata T, Whitman S, Johnson TA, Stessman CC, Loo CP, Lobkovsky E, Clardy J, Crews P, Holman TR. J. Nat. Prod 2003;66:230–235. [PubMed: 12608855]
10. Pina IC, Sanders ML, Crews P. J. Nat. Prod 2003;66:2–6. [PubMed: 12542334]
11. Ueda KUT, Siwu ERO, Kita M, Uemura D. Chem. Lett 2005;34:1530–1531.
12. Ravi BN, Perzanowski HP, Ross RA, Erdman TR, Scheuer PJ, Finer J, Clardy J. Pure Appl. Chem 1979;51:1893–1900.
13. Urban S, Capon RJ. J. Nat. Prod 1996;59:900–901.
14. Ueda K, Ogi T, Sato A, Siwu ERO, Kita M, Uemura D. Heterocycles 2007;72:655–663.
15. Nasu SS, Yeung BKS, Hamann MT, Scheuer PJ, Kelly-Borges M, Goins K. J. Org. Chem 1995;60:7290–7292.
16. Hamann MT, Scheuer PJ, Kelly-Borges M. J. Org. Chem 1993;58:6565–6569.
17. Dale JA, Mosher HS. J. Am. Chem. Soc 1973;95:512–519.
18. Ohtanoi IKT, Kashman Y, Kakisawa H. J. Am. Chem. Soc 1991;113:4092–4096.
19. Rubio, BK. Bioactive Natural Products for Global Health from Papua New Guinea Marine Sponges. Santa Cruz: University of California; 2008.
20. Carter GW, Young PR, Albert DH, Bouska J, Dyer R, Bell RL, Summers JB, Brooks DW. J. Pharmacol. Exp. Ther 1991;256:929–937. [PubMed: 1848634]

21. Whitman S, Gezginci M, Timmermann BN, Holman TR. J. Med. Chem 2002;45:2659–2661. [PubMed: 12036375]
22. Blunt, J.; Munro, M. Marinlit. Christchurch, NZ: University of Cantebury; 2009 Feb.
23. Kraus GA, Nguyen T, Bae J, Hostetter J, Steadham E. Tetrahedron 2004;60:4223–4225.
24. Ishibashi H, Ishihara K, Yamamoto H. J. Am. Chem. Soc 2004;126:11122–11123. [PubMed: 15355072]
25. Asche C, Frank W, Albert A, Kucklaender U. Bioorg. Med. Chem 2005;13:819–837. [PubMed: 15653349]
26. Alvarez-Manzaneda EJ, Chahboun R, Perez IB, Cabrera E, Alvarez E, Alvarez-Manzaneda R. Org. Lett 2005;7:1477–1480. [PubMed: 15816731]
27. Gansaeuer A, Rosales A, Justicia J. Synlett 2006:927–929.
28. Gansaeuer A, Justicia J, Rosales A, Worgull D, Rinker B, Cuerva JM, Oltra JE. Eur. J. Org. Chem 2006:4115–4127.
29. Barrero AF, Quilez del Moral JF, Mar Herrador M, Arteaga P, Cortes M, Benites J, Rosellon A. Tetrahedron 2006;62:6012–6017.
30. Alvarez-Manzaneda EJ, Chahboun R, Cabrera E, Alvarez E, Haidour A, Ramos JM, Alvarez-Manzaneda R, Hmamouchi M, Bouanou H. J. Org. Chem 2007;72:3332–3339. [PubMed: 17388632]
31. Pritchard RG, Sheldrake HM, Taylor IZ, Wallace TW. Tetrahedron Lett 2008;49:4156–4159.
32. Hooper, JNA.; Van Soest, RWM. *Hyrtios*, Dachassaing & Michelotti. In: Hooper, JNA.; Van Soest, RWM.; Willenz, P., editors. System Porifera. Vol. Vol. 1. New York: Kluwer Academic / Plenum Publishers; 2002. p. 1030-1031.
33. Sperry S, Valeriote FA, Corbett TH, Crews P. J. Nat. Prod 1998;61:241–247. [PubMed: 9514009]
34. Robinson SJ, Tenney K, Yee DF, Martinez L, Media JE, Valeriote FA, van Soest RWM, Crews P. J. Nat. Prod 2007;70:1002–1009. [PubMed: 17559267]
35. Chen XS, Brash AR, Funk CD. Eur. J. Biochem 1993;214:845–852. [PubMed: 8319693]
36. Pande AHMD, Nemec KN, Qin S, Tan S, Tatulian SA. Biochem 2004;43:14653–14666. [PubMed: 15544336]

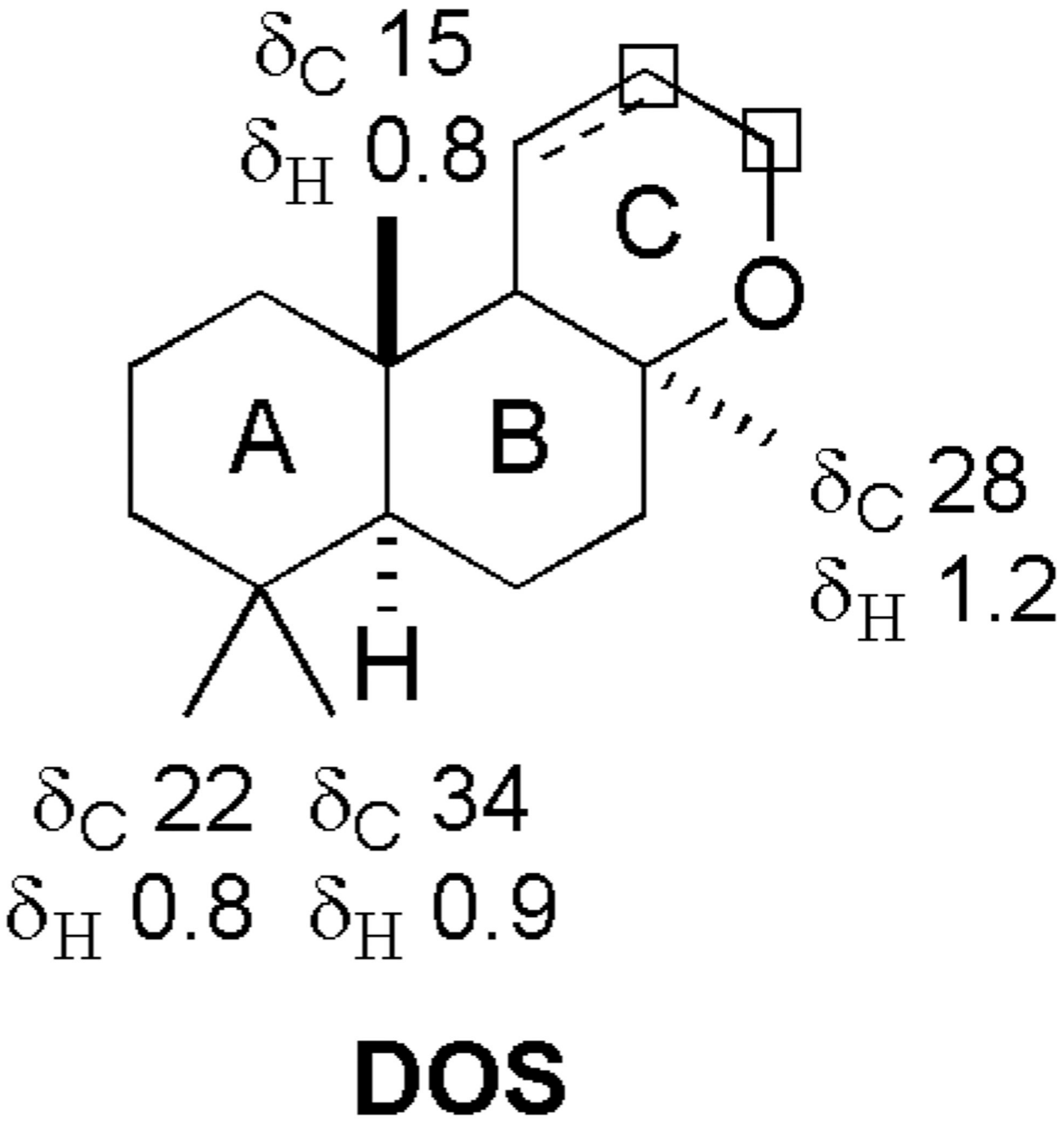

Figure 1.
ABC ring drimane oxygenated shikimate (**DOS**) core (□ indicating nonterpene portion) with corresponding diagnostic CH_3 δ_C/δ_H NMR data.

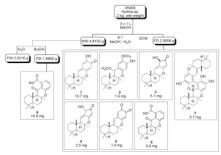

Figure 2.
Isolation scheme for compounds **1 – 7**.

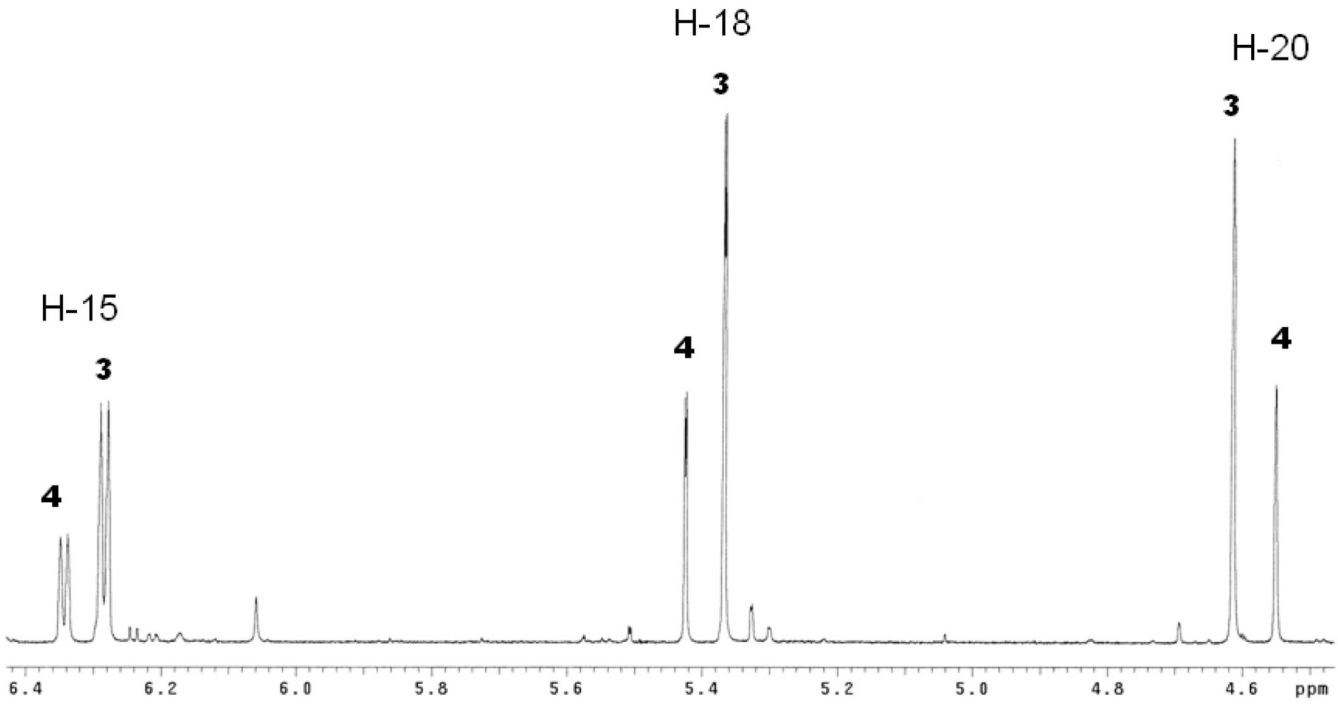

Figure 3.
Downfield ^{1}H NMR (600 MHz, $CDCl_3$) spectra of FD L2 H5 with **3** and **4** in a 2:1 ratio respectively.

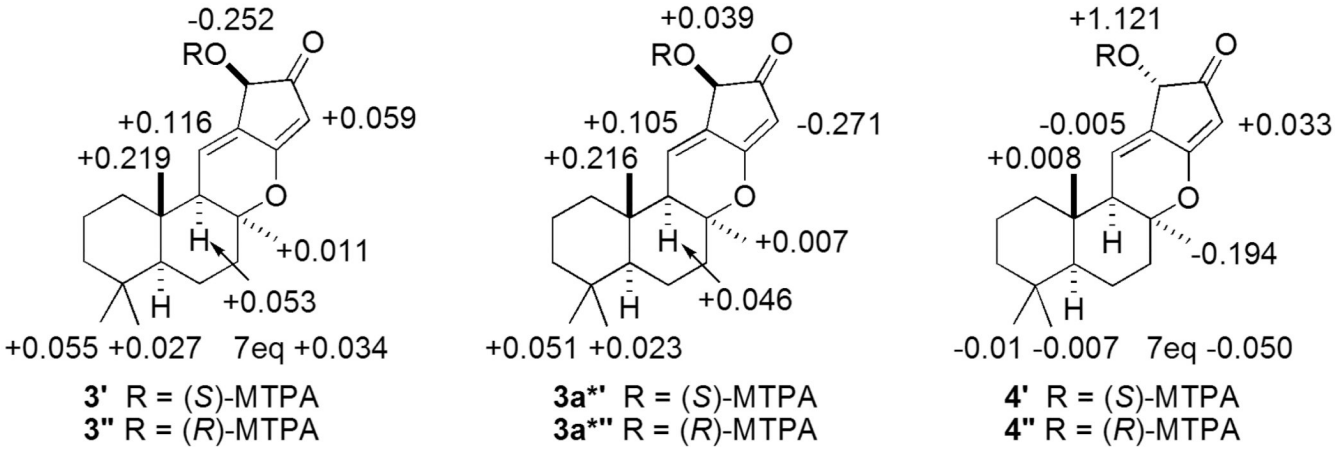

Figure 4.
Modified Mosher's method analysis, $\Delta\delta^{SR}$, of **3, 3a**, and **4**. *Literature data of $\Delta\delta^{SR}$ at C-18 and C-20 of **3a** were inadvertently switched in the original publication.[14]

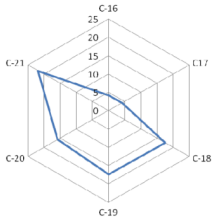

Figure 5.
^{13}C NMR Δδ shift differences between 15-oxo-puupehenoic acid (**6**) and 15-oxo-puupehenol (**8**), with $\Delta\delta_C$ differences < 2 ppm not included.

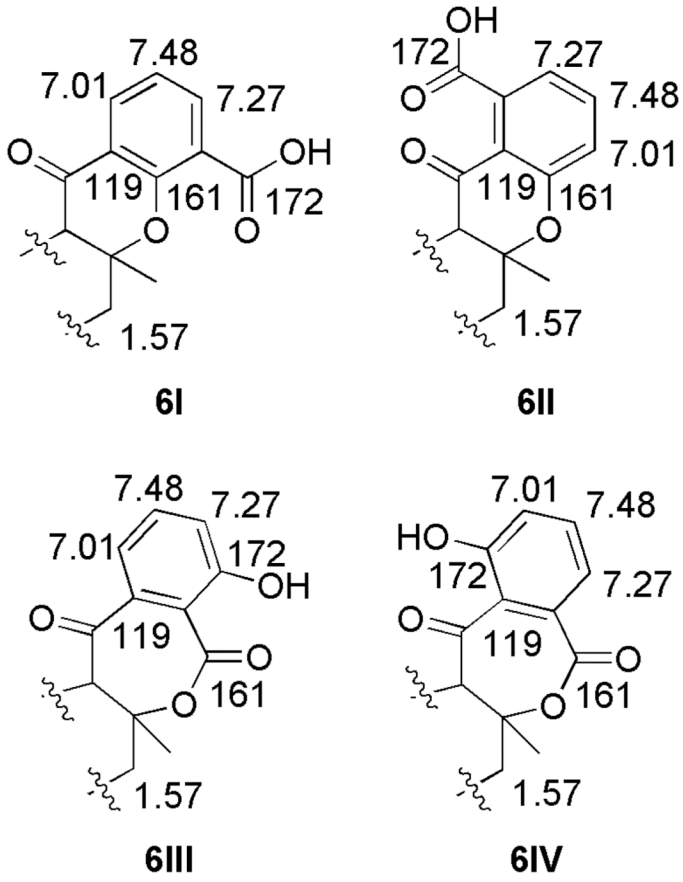

J_{HC} gHMBC correlations	Fit of working structures to correlations			
δ_H to δ_C	**6I**	**6II**	**6III**	**6IV**
1.57 to 161*	yes	yes	yes	yes
7.01 to 119‡	yes	yes	yes	yes
7.27 to 119‡	no	yes	no	yes
7.48 to 161‡	no	yes	no	no

Figure 6.
Analysis of working structures for the CD rings of **6** based on J_{HC} correlations expected for each working structure. $^{*4}J_{HC}$ and $^{‡2,3}J_{HC}$ correlations requiring $\delta_{H/C}$ placement as shown.

Table 1

^{1}H, ^{13}C, gCOSY, gHMBC and gNOESY NMR Data of 15-Oxo-puupehenoic acid (**6**) in $CDCl_3$ at 600 MHz (^{1}H) and 150 MHz (^{13}C)

pos #	δ_C, type[b]	δ_H, m., (*J* [Hz])	gCOSY	gHMBC (^{1}H to ^{13}C)	NOESY
1 ax	40.0, CH_2	1.21, m	2	2, 10	5, 9
1 eq		1.62, m			
2	18.1, CH_2	1.66, m	1, 3	1	
3 ax	41.4, CH_2	1.18, m	2	1, 4, 12	1ax, 5, 11
3 eq		1.42, m		2	
4	33.4, qC				
5	54.2, CH	0.91, dd (11.5, 2.5)	6	4, 6, 14	1ax, 9, 11
6	18.3, CH_2	1.44, m	5, 7	7	
7 ax	39.5, CH_2	1.57, ddd (14, 11, 2.5)	6	5, 9, 17[a]	9
7 eq		2.26, dt (14, 2.5)		8, 13	
8	80.4, qC				
9	64.9, CH	2.04, s		1, 5, 10, 13, 15, 16	1ax, 5, 7 ax, 13
10	38.7, qC				
11	33.7, CH_3	0.92, s		3, 5, 12	5, 9
12	21.9, CH_3	0.84, s		3, 11	
13	26.4, CH_3	1.22, s		7, 8, 9	9
14	15.4, CH_3	0.88, s		1, 9, 10	
15	196.2, qC				
16	119.2, qC				
17	161.0, qC				
18	121.3, CH	7.01, dd (8, 1.5)	19	15[a], 16, 17, 20	20
19	135.3, CH	7.48, dd (8, 7.5)	18, 20	16[a], 17, 20, 21, 22[a]	19, 21
20	122.2, CH	7.27, dd (7.5, 1.5)	19	16, 17[a], 18, 19, 22	20
21	132.6, qC				
22	171.9, qC				

[a] gHMBC at 600 MHz optimized for 5 Hz correlations in $CDCl_3$.

[b] Carbon type determined by a DEPT NMR experiment.

Table 2

Comparison of hLO IC_{50} Values (μM) of Natural Products and Standards

Compound	12-hLO	15-hLO-1	5-hLO	12-hLO/5-hLO	15-hLO/5-hLO
1	22 ± 3	6.0 ± 1	0.68 ± 0.1	32	9
3	> 150	> 150	> 50	~ 3	~ 3
5	18 ± 2	7.0 ± 1	4.6 ± 2	4	1.5
6	> 150	> 150	> 150	n.s.	n.s.
9	> 50	19 ± 3	0.45 ± 0.08	> 111	42
10	7.9 ± 0.8	4.7 ± 0.3	14 ± 2	0.6	0.3
11	31 ± 3	16 ± 3	18 ± 8	2	0.9
12	5.9 ± 0.8	1.1 ± 0.1	0.11 ± 0.03	54	11
13	Active [*,**]	NA [*]	0.5 ± 0.1 [*]	> 200	> 200

[*] Data from literature.[20]

[**] 19% inhibition at 100 μM.